Supplementary material for "Extremal connectedness of hedge funds"

Linda Mhalla*
HEC Lausanne, University of Lausanne, Switzerland

Julien Hambuckers
University of Liège – HEC Management School, Belgium

Marie Lambert
University of Liège – HEC Management School, Belgium

November 25, 2021

1 Description of the hedge funds data

This section supplements Section 3.1 in the paper.

1.1 Filtering of the data

Here, we detail the preprocessing of the original dataset extracted from the Hedge Fund Research (HFR) database. First, we remove funds not reporting net-of-fees returns in a monthly basis, or with partial quarterly observations. Second, we remove funds with missing historical data (returns, total assets, minimum investment) and/or missing observations of their fund specific factors, e.g., investment style, management and incentive fees, country of residence, and leverage. Additionally, we only keep funds for which the reported country of residence belongs to one of the following developed countries: Australia, Austria, Belgium, Canada, Czech Republic, Denmark, Finland, France, Germany, Greece, Ireland, Israel, Italy, Japan, Luxembourg, Netherlands, New Zealand, Norway, Portugal, Spain, Sweden, Switzerland, United States of America., and United Kingdom. This step ensures the availability of the macroeconomic data for each of the resulting funds. Similarly, we remove funds that are reporting for less than 24 months. Moreover, to avoid double counting and inconsistent reporting standards, we remove funds of funds, and funds with an inception date prior to December 1989. Finally, we only keep returns starting in January 1994, first date at which some of the explanatory variables used in the multivariate analysis are available. Our database stops in May 2017.

1.2 Descriptive statistics

Descriptive statistics of the historical returns for each investment style are reported in Table 1. We observe important differences in all aspects of their respective distributions, especially in the skewness and kurtosis dimensions.

*Linda Mhalla, HEC Lausanne, University of Lausanne, CH-1015 Lausanne, Switzerland. E-mail: linda.mhalla@unil.ch

Acknowledgments: L. Mhalla (LM) acknowledges the support of the Swiss National Science Foundation (grant P2GEP2_181062). J. Hambuckers (JH) acknowledges the financial support of the National Bank of Belgium. Marie Lambert acknowledges the support of the Deloitte Chair of Financial Management and Corporate Valuation at University of Liège, HEC Liège, (Belgium). Parts of the research for this paper were conducted while LM was affiliated to HEC Montréal (Canada) and JH to the University of Göttingen (Germany), Chair of Statistics.

Inv. Style	Mean	Std.	Skew.	Kurt.	# Funds	# Obs.
Conv. Arb.	0.07	0.16	-2.01	56.54	387	31,044
Dist./Rest.	0.08	0.14	-0.37	58.58	222	20,802
Eq. M. Neut.	0.06	0.11	-0.33	25.61	566	42,097
F. Inc. Arb.	0.07	0.11	-2.66	67.86	660	54,502
Glob. Trad.	0.07	0.18	0.78	17.92	1,305	111,085
L/S Eq.	0.09	0.19	0.35	20.54	3,205	280,966
Man. Fut.	0.07	0.19	1.37	27.64	406	31,555
Merg. Arb.	0.07	0.08	1.09	44.97	122	11,702
Mult. Str.	0.07	0.12	0.09	73.51	421	35,951
Others (ED)	0.10	0.16	0.59	29.83	471	42,315
Sh. Bias	0.02	0.18	0.40	6.85	42	2,919
Y. Alt.	0.09	0.17	-0.39	15.69	117	8,855

Table 1: Descriptive statistics of the panel of hedge funds, over the period January 1994–May 2017 for a given investment style. Mean and variance of the returns are expressed in yearly equivalent rates.

2 Marginal and dependence modeling of investment styles

This section supplements Section 3.2 and 3.3 in the paper.

2.1 Marginal tail risk of hedge funds

We report in Tables 2 and 3 the estimated regression coefficients of the dynamic Generalized Pareto models, obtained without the regularization step. That is, the maximum likelihood estimates of the regression coefficients of the models for $\sigma(\mathbf{x}_0^\sigma)$ and $\xi(\mathbf{x}_0^\xi)$; see Equations (3)–(4) in the paper.

These results are difficult to interpret since we have a large number of candidate explanatory variables. To tackle this issue in our main analysis, we use the LASSO-based penalization procedure of Hambuckers et al. (2018). We display the estimated regression coefficients $\hat{\boldsymbol{\beta}}_0^\sigma$ and $\hat{\boldsymbol{\beta}}_0^\xi$ obtained with the LASSO procedure in Tables 4 and 5, respectively. We do not report any standard errors, since we should technically account for post-selection inference, a complex question beyond the scope of this paper. Usual standard errors based on the observed Fisher information matrix for an additional unpenalized step are available upon request.

Finally, to stress the robustness of our findings, we compare the results obtained with the post-LASSO estimator and a pre-test approach where we only select significant covariates at the 1% test level, using a BIC criterion. A summary is displayed in Figure 1, where we report $1-BIC(\text{pre-test})/BIC(\text{post-LASSO})$, with negative values indicating a better BIC for the post-LASSO estimator. We see that, for all investment styles, either the LASSO does much better (up to 3.5% decrease in BIC), or is equivalent (at most 0.2% larger). These results point in the direction of a good selection procedure obtained with the LASSO approach.

2.2 Hedge funds connectedness

Figure 2 displays the mean extremal connectedness measures conditional on the market factors (`MSCI`, `EPU`, `FSI`) being larger than their third respective quartiles. This figure highlights the existence of changes in extremal connectedness under different market stress conditions.

3 Marginal tail risk of banks and extremal connectedness with hedge funds

The focus of the paper is on extremal connectedness *within* the hedge fund sector. However, in the perspective of quantifying the contribution of hedge funds to systemic risks, we investigate in Subsection 3.4.3 of the main manuscript the extremal connectedness *between* hedge funds

σ	Conv. arb.	Distr./Rest.	Eq. mar. neut.	F. inc. arb.	Glob. trad.	Long/Short eq.	Man. Fut.	Merg. arb.	Multi-strat.	Other	Short bias	Yield alt.
Cst	1.480	1.211	0.847	1.015	1.259	1.472	1.417	0.688	1.040	1.349	1.193	1.492
$\lvert R_{t-1} \rvert$	0.420	0.301	0.179	0.320	0.309	0.353	0.327	0.161	0.305	0.426	0.226	0.111
IncFee	0.159	0.051	0.060	-0.033	0.156	-0.004	0.050	0.078	-0.085	0.029	-0.067	-0.117
ManFee	0.170	0.023	-0.079	0.068	0.050	0.037	-0.026	0.016	0.084	-0.016	-0.071	-0.124
TotAss	-0.024	-0.110	0.009	-0.032	-0.067	-0.077	-0.107	0.133	-0.073	-0.051	0.064	-0.067
IntRateST	0.084	0.047	0.213	0.137	-0.177	-0.016	0.046	0.077	0.044	-0.104	0.033	-0.175
IntRateLT	0.183	0.026	0.001	0.091	0.105	0.081	0.044	0.004	-0.064	0.024	-0.023	0.054
IndProd	-0.084	-0.117	0.000	-0.027	-0.057	0.031	0.014	0.088	0.065	-0.029	-0.079	-0.094
StockVol	-0.002	0.007	0.148	0.133	0.026	-0.025	0.053	0.075	0.006	-0.125	-0.018	0.002
UnempRate	0.019	-0.017	-0.074	-0.054	-0.080	-0.029	0.004	0.016	0.024	0.001	0.040	0.016
Leverage	0.046	-0.017	0.039	0.008	-0.020	-0.001	0.018	-0.023	-0.011	-0.045	-0.020	0.009
PTFSBD	0.074	0.060	0.040	0.044	0.014	0.047	0.091	0.143	-0.036	0.036	0.032	0.072
PTFSFX	0.022	0.083	0.038	0.193	0.018	-0.019	-0.073	0.148	0.091	-0.070	-0.138	-0.022
PTFSCOM	0.282	0.115	0.107	0.157	0.062	0.150	0.127	0.096	0.052	0.154	-0.046	-0.048
EMF	-0.391	-0.151	-0.432	-0.174	-0.107	-0.325	-0.020	-0.166	-0.276	-0.430	0.068	-0.318
ESF	0.225	-0.048	0.303	0.155	0.038	0.128	0.021	-0.024	0.076	0.191	0.036	-0.126
BD10RET	-0.223	0.050	-0.218	-0.037	0.099	0.009	-0.076	-0.160	-0.001	0.056	-0.036	0.121
BAAMTSY	0.065	-0.083	-0.017	-0.253	0.025	-0.033	-0.007	-0.190	-0.237	0.073	-0.104	-0.273
SMB	-0.135	0.039	-0.189	-0.123	-0.120	-0.131	-0.068	-0.020	-0.162	-0.271	0.028	-0.082
HML	0.041	0.041	-0.054	0.045	-0.010	0.059	0.087	0.003	0.058	-0.034	-0.072	0.081
MOM	-0.151	-0.041	-0.224	0.007	-0.033	-0.090	-0.067	-0.022	-0.072	-0.119	-0.017	0.004

Table 2: Estimated regression parameters $\boldsymbol{\beta}_0^{\sigma}$ for the dynamic generalized Pareto regression model, obtained with the classical MLE procedure.

ξ	Conv. arb.	Distr./Rest.	Eq. mar. neut.	F. inc. arb.	Glob. trad.	Long/Short eq.	Man. Fut.	Merg. arb.	Multi-strat.	Other	Short bias	Yield alt.
Cst	0.137	0.125	0.047	0.096	0.081	0.046	0.008	0.013	0.103	0.076	0.257	-0.066
$\lvert R_{t-1} \rvert$	-0.178	0.046	0.023	-0.097	-0.042	-0.049	0.006	0.012	0.034	-0.074	-0.057	-0.048
IncFee	0.095	0.068	-0.058	0.012	-0.042	0.024	-0.052	-0.078	0.143	0.016	0.024	0.085
ManFee	-0.072	0.014	0.107	0.093	-0.021	-0.004	0.009	0.080	0.021	-0.005	0.016	0.094
TotAss	-0.052	-0.031	-0.097	0.002	0.008	0.019	0.008	-0.046	-0.017	-0.006	-0.062	0.012
IntRateST	-0.126	-0.004	-0.350	0.022	0.076	0.007	-0.096	-0.008	-0.002	0.176	0.043	-0.065
IntRateLT	0.102	-0.020	0.197	0.271	-0.060	-0.052	0.095	0.063	0.019	-0.078	0.060	-0.051
IndProd	0.035	0.021	0.004	-0.011	0.038	-0.048	-0.037	0.046	-0.099	0.030	0.058	0.090
StockVol	0.047	0.045	-0.121	-0.026	-0.035	-0.031	-0.043	0.056	0.004	0.107	-0.026	-0.117
UnempRate	-0.128	-0.013	0.012	0.008	0.056	0.024	0.013	-0.141	-0.093	0.068	-0.066	-0.042
Leverage	-0.005	-0.001	0.008	-0.055	-0.042	-0.018	-0.059	-0.078	0.020	-0.029	-0.036	-0.030
PTFSBD	-0.017	-0.007	0.007	-0.052	0.016	0.014	-0.117	-0.061	-0.023	-0.036	0.032	-0.120
PTFSFX	-0.037	-0.080	-0.081	-0.088	0.017	-0.040	0.142	-0.116	-0.118	0.005	0.063	-0.124
PTFSCOM	-0.128	-0.050	0.096	-0.070	0.005	-0.042	0.018	-0.037	0.007	-0.051	0.083	0.013
EMF	0.068	0.061	0.240	0.070	0.011	0.097	-0.014	0.051	0.056	0.155	-0.065	0.117
ESF	-0.114	0.003	-0.147	-0.142	-0.047	-0.045	-0.038	-0.039	0.037	-0.071	-0.008	0.084
BD10RET	-0.093	0.003	0.219	-0.147	-0.029	0.035	-0.079	0.060	-0.013	-0.002	0.059	0.041
BAAMTSY	-0.022	0.077	-0.037	0.076	-0.015	0.052	0.076	0.067	0.055	-0.017	0.084	-0.011
SMB	0.006	0.025	0.082	0.108	0.046	0.047	0.023	0.064	0.040	0.089	0.009	0.029
HML	0.120	-0.022	0.000	-0.052	-0.003	0.003	-0.061	-0.042	-0.039	-0.010	-0.023	0.106
MOM	0.089	0.027	0.049	0.025	0.011	0.034	-0.001	-0.043	0.033	0.086	0.059	0.029

Table 3: Estimated regression parameters $\boldsymbol{\beta}_0^{\xi}$ for the dynamic generalized Pareto regression model, obtained with the classical MLE procedure.

σ	Conv. arb.	Distr./Rest.	Eq. mar. neut.	F. inc. arb.	Glob. trad.	Long/Short eq.	Man. Fut.	Merg. arb.	Multi-strat.	Other	Short bias	Yield alt.
Cst	1.468	1.234	0.834	1.007	1.253	1.479	1.367	0.705	1.016	1.345	1.256	1.603
$\lvert R_{t-1}\rvert$	0.304	0.187	0.153	0.214	0.220	0.321	0.243	0.145	0.258	0.250	0.148	0
Incfees	0.153	0	0	0	0.055	0	0	0	0	0	0	0
ManFees	0.081	0	0	0.070	0	0.022	0	0	0.033	0	0	0
TotAss	-0.045	0	0	0	0	-0.025	0	0	0	0	0	0
IntRateST	0	0	0	0.077	0	0.036	0	0	0	0.014	0	0
IntRateLT	0	0	0.033	0.186	0	0	0	0	0	0	0	0
IndProd	0	0	0	-0.012	0	0	0	0	-0.022	-0.004	0	-0.035
StockVol	0	0	0	0.016	0	-0.029	0	0	0	0	0	0
UnempRate	0	0	0	0	0	-0.005	0	0	0	0	0	0
Leverage	0	0	0	0	0	-0.004	0	0	0	0	0	0
PTFSBD	0	0	0.019	0	0	0.042	0	0.086	0	0	0	0
PTFSFX	0.027	0	0	0.129	0	0	0	0.033	0	0	0	0
PTFSCOM	0.222	0	0.126	0.083	0	0.129	0.084	0	0	0.065	0	0
EMF	-0.225	-0.110	-0.135	-0.077	0	-0.245	0	-0.054	-0.124	-0.128	0	-0.108
ESF	0	0	0	0	0	0.027	0	0	0	0	0	0
BD10RET	0	0	0	0	0	0.035	0	0	0	0	0	0
BAAMTSY	0	0	-0.046	-0.225	0	0	0	-0.056	-0.107	0	0	-0.180
SMB	-0.062	0	0	0	0	-0.039	0	0	-0.030	-0.083	0	0
HML	0.084	0	0	0	0	0.059	0	0	0	0	0	0
MOM	-0.049	0	-0.064	0	0	-0.032	0	0	0	0	0	0

Table 4: Estimated regression parameters $\boldsymbol{\beta}_0^{\sigma}$ for the dynamic generalized Pareto regression model, obtained with the LASSO procedure.

ξ	Conv. arb.	Distr./Rest.	Eq. mar. neut.	F. inc. arb.	Glob. trad.	Long/Short eq.	Man. Fut.	Merg. arb.	Multi-strat.	Other	Short bias	Yield alt.
Cst	0.172	0.179	0.085	0.127	0.091	0.040	0.085	0.021	0.180	0.114	-0.052	-0.033
$\lvert R_{t-1} \rvert$	0	0	0	0	0	-0.034	0	0	0	0	0	0
IncFee	0	0	0	0	0	0.026	0	0	0	0	0	0
ManFee	0	0	0	0	0	0	0	0.093	0	0	0	0
TotAss,	0	0	-0.065	0	0	0	0	0	0	0	0	0
IntRateST	0	0	0	0	0	0	0	0	0	0	0	0
IntRateLT	0	0	0	0	0	0	0	0	0	0	0	0
IndProd	0	0	0	0	0	-0.014	0	0	0	0	0	0
StockVol	0	0	0	0	0	-0.009	0	0	0	0	0	0
UnempRate	0	0	0	0	0	0	0	0	0	0	0	0
Leverage	0	0	0	0	-0.031	-0.006	0	-0.047	0	0	0	0
PTFSBD	0	0	0	0	0.015	0	0	0	0	0	0	0
PTFSFX	0	0	0	0	0.020	-0.041	0	0	0	0	0	0
PTFSCOM	0	0	0	0	0.025	-0.023	0	0	0	0	0	0
EMF	0	0	0	0	-0.029	0.052	0	0	0	0	0	0
ESF	0	0	0	0	-0.023	0	0	0	0	0	0	0
BD10RET	0	0	0	0	0	0	0	0	0	0	0	0
BAAMTSY	0	0	0	0	0	0.023	0	0	0	0	0	0
SMB	0	0	0	0	0	0	0	0	0	0	0	0
HML	0	0	0	0	0	0	0	0	0	0	0	0
MOM	0	0	0	0	0	0	0	0	0	0	0	0

Table 5: Estimated regression parameters $\boldsymbol{\beta}_0^{\xi}$ for the dynamic generalized Pareto regression model, obtained with the LASSO procedure.

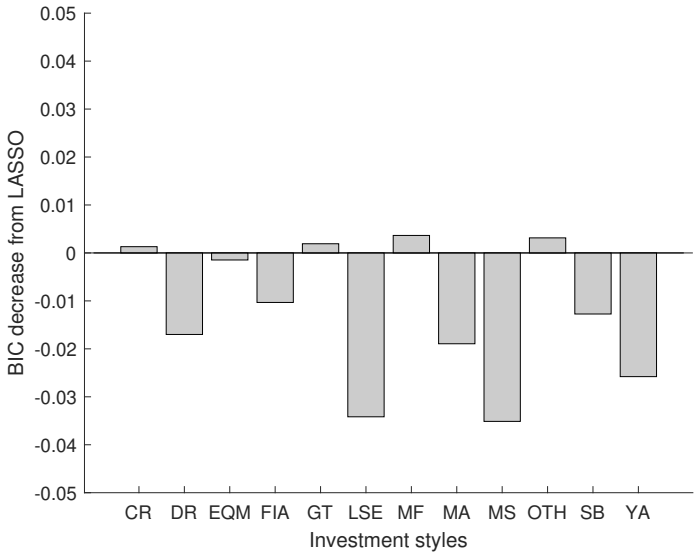

Figure 1: Relative BIC for models obtained either with a pre-test estimator (i.e. a maximum likelihood estimator of the GP regression model, fitted with the subset of covariates for which the p-value of the full model is smaller than 0.01), or a post-LASSO estimator.

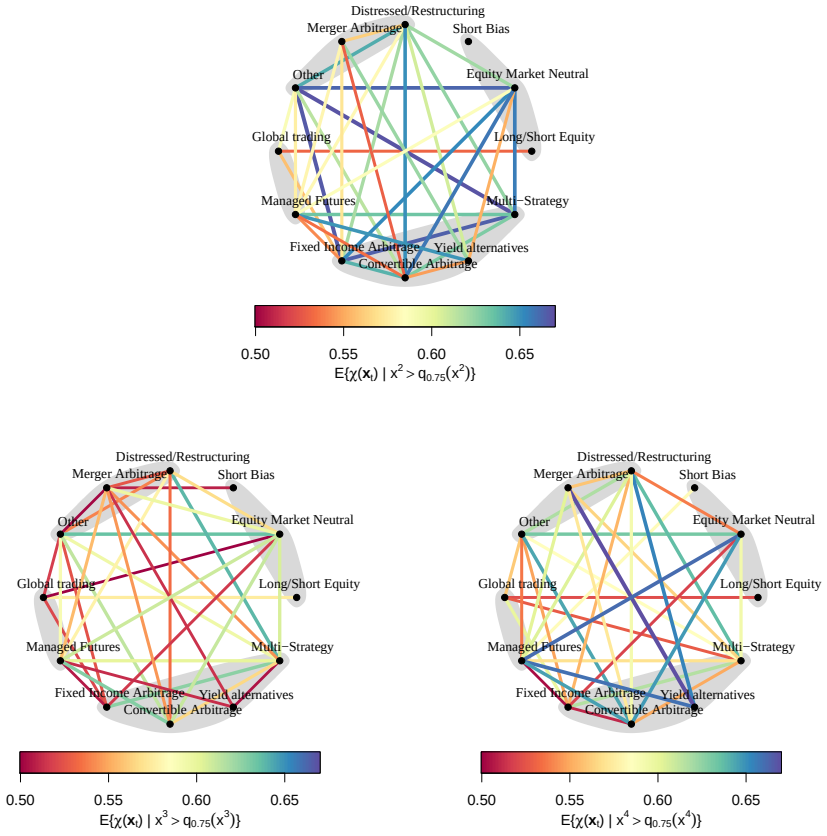

Figure 2: Empirical mean of the pairwise conditional tail coefficient $\chi(\mathbf{x}_t)$ conditional on the following market factors exceeding their highest quartile: `MSCI` (top), `EPU` (bottom left), and `FSI` (bottom right). For better visibility, edges with values exceeding the median of all edges' values are removed. The width of the edges is proportional to the estimated value.

and the classical financial system. To do so, we employ the same approach as defined in the Methodology section of the paper, although slightly modified. In the present section, we provide more details of our computations.

3.1 Bank data

To build a representative sample of the financial system, we collect daily (log) returns and market values for 29 international banks listed in developed countries, over the period 01/1994–05/2017 and [1]. The full list is given in Table 6. Twenty of these banks are classified by the Financial Stability Board as being globally systemically important institutions, whereas the other nine banks are major ones in terms of total assets. One bank is also listed as an insurer (AXA) by the data provider, whereas three banks fall in the investment bank/broker-dealer category as well (Goldman Sachs, Morgan Stanley, and Credit Suisse). When market value is missing for a particular day, we use the value registered the day before. To assess the robustness of our findings to the choice of this sample, we repeat our analysis with a sample composed solely of investment banks/broker-dealers in the next section.

United States	Europe	Canada & Japan
Citigroup (C)	Standard Chartered (STAN)	Bank of Montreal (BMO)
JP Morgan Chase (JPM)	Barclays (BCS)	Bank of Nova Scotia (BNS)
Bank of America (BAC)	HSBC, Lloyds (LYG)	Imperial Bank of Commerce (CM)
Bank of NY Mellon (BK)	Credit Suisse (CS)	Royal Bank of Canada (RY)
Goldman Sachs (GS)	Commerzbank (CBK)	Toronto Dominion (TD)
Morgan Stanley (MS)	Deutsche Bank (DB), ING	Mitsubishi UFJ (MUFJ)
State Street (STT)	Soc. Gen. (GLE), AXA	-
Westpac Bank. Corp. (WBK)	BNP Paribas (BNP), Int. Sanpaolo (ISP)	-
Wells Fargo (WFC)	Santander (SAN), BBVA	-

Table 6: List of banks, split per listing origins.

3.2 Marginal tail risk of banks

Similarly to hedge funds, we first need to model the distribution of extremely negative returns and filter out the dynamics in the tail. We do so with the dynamic GP regression approach described in Section 2.1. However, we face the challenge that our pool of banks is much narrower than the one of hedge funds, which would yield very few extreme observations per month if the analysis is based on monthly data. To bypass this issue, we use *daily* data instead. Our initial sample consists therefore of the daily (log) returns of all banks, pooled together. This initial sample consists of 167,689 observations (Figure 3, panel (a)).

To select our final sample of exceedances, we apply the same threshold estimation method based on quantile regression as used for our main analysis, such that we have roughly 5% of the largest losses in a given month above the threshold. In essence, this consists of estimating a quantile regression model with time (expressed in month) as a covariate. Our final sample of exceedances consists of the 8,366 observations larger than the time-varying threshold. Their histogram is displayed in Figure 3, panel (b).

To control for common risk exposures and remove the marginal tail dynamic, we fit the dynamic GPD model on the exceedances. We use the following set of covariates $\mathbf{x}_0^{banks}$ in both the shape and the scale parameters, motivated by the approach of Agarwal et al. (2017) and Hale & Lopez (2019):

$$\{|R_{t-1}|, \texttt{BankID},$$
$$\texttt{PTFSBD}_t, \texttt{PTFSFX}_t, \texttt{PTFSCOM}_t, \texttt{EMF}_t, \texttt{ESF}_t, \texttt{BD10RET}_t, \texttt{BAAMTSY}_t,$$
$$\texttt{MKT}_t, \texttt{SMB}_t, \texttt{HML}_t, \texttt{MOM}_t\}.$$

$|R_{t-1}|$ is the absolute lagged returns, used to control for bank-specific heteroscedasticity. BankID is a bank-specific fixed effect. $\texttt{PTFSBD}_t$, $\texttt{PTFSFX}_t$, $\texttt{PTFSCOM}_t$, $\texttt{EMF}_t$, $\texttt{ESF}_t$, $\texttt{BD10RET}_t$ and $\texttt{BAAMTSY}_t$

[1] The data are retrieved from Capital IQ.

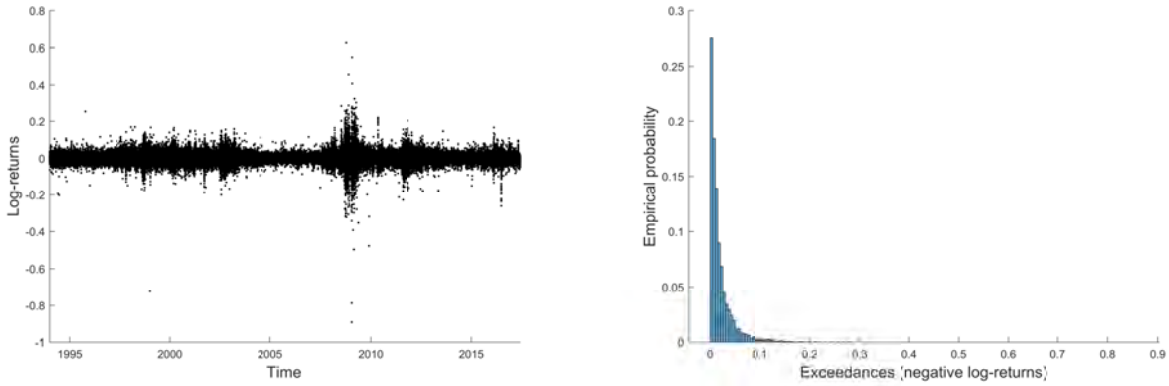

(a) (b)

Figure 3: (a) Initial (pooled) sample of the daily log-returns for 29 major banks in developed countries (USA, Canada, Europe, and Japan), over the period 01/1994 - 05/2017. (b) Histogram of the loss exceedances (top 5%) above a time-varying threshold, computed with a quantile regression approach.

are the seven factors of Fung & Hsieh (2004). Finally, $\texttt{MKT}_t$, $\texttt{SMB}_t$, $\texttt{HML}_t$ and $\texttt{MOM}_t$ are the four factors (market, size, value, and momentum) of Carhart (1997) and Fama & French (1993). We use our LASSO approach to estimate the model and select the relevant covariates. The fixed effects are not subject to penalization and are included by default in the model. Our results are the following: for the shape parameter, all covariates are excluded from the final model. On the contrary, for the scale parameter, they are all kept in the model except $\texttt{EMF}_t$ and $\texttt{PTFSFX}_t$. Estimated parameters are reported in Table 7. The QQ-plot for the exceedances reveals a good fit (Figure 4, panel (a)). Similarly to what is done for the hedge funds' investment styles, we rely on our model to construct the weighted VaR at level $\alpha = 99\%$, over time and across all banks, using the daily relative market values as weights (instead of the total assets). Monthly averages of this quantity are displayed in Figure 4, panel (b). We see an important peak during the financial crisis, as well as after the 9/11 terrorist attacks.

3.3 Extremal connectedness between funds and banks

Finally, using the estimated distribution combining the empirical distribution and the dynamic GPD, we transform the banks' negative returns to the unit-Fréchet scale. For each month, we have therefore around 600 observations from which the largest ones are matched with the largest monthly hedge funds' (rescaled) losses to form pairs of losses[2]. Then, the dynamic extremal connectedness between banks and funds is obtained by fitting the Hüsler–Reiss parametric family (Hüsler & Reiss 1989) to the pairs exceeding a large radial threshold, modeled through a parametric quantile regression at the 95 % level. In Figure 5, we display the average connectedness between banks and the various hedge funds' investment styles over the entire period of analysis. The estimate $\hat{\chi}_t^{banks,l}$ over time can be found in Figure 6.

4 Marginal tail risk of broker-dealers and extremal connectedness with hedge funds

To give additional insights on the connectedness of funds with the financial system, we repeat our analysis with a sample of financial institutions registered solely as broker-dealers.

4.1 List of selected broker-dealers

This section details the selection process of the broker-dealers' sample with daily stock price and market value data obtained from Capital IQ. To select our sample, we apply the following filters:

[2]This matching approach implies that the extremal connectedness is assumed constant within a given month.

Factor	$\hat{\boldsymbol{\beta}}_0^{\sigma}$ (MLE)	$\hat{\boldsymbol{\beta}}_0^{\sigma}$ (LASSO)	$\hat{\boldsymbol{\beta}}_0^{\xi}$ (MLE)	$\hat{\boldsymbol{\beta}}_0^{\xi}$ (LASSO)
BAC	-3.961	-3.943	0.139	0.110
BBVA	-0.239	-0.281	-0.062	0.008
BCS	-0.139	-0.157	-0.003	0.033
BK	-0.280	-0.282	0.017	0.027
BMO	-0.407	-0.441	-0.193	-0.137
BNP	-0.022	-0.078	-0.173	-0.090
BNS	-0.494	-0.516	-0.145	-0.114
CBK	0.037	0.016	-0.096	-0.056
C	-0.057	-0.047	0.015	0.004
CM	-0.465	-0.491	-0.038	0.015
CS	-0.009	-0.029	-0.093	-0.048
DB	-0.008	-0.036	-0.139	-0.089
GLE	0.083	0.036	-0.143	-0.068
GS	-0.218	-0.255	-0.021	0.030
HSBC	-0.197	-0.189	-0.076	-0.086
ING	0.056	0.023	0.017	0.090
ISP	0.023	-0.016	-0.044	0.006
JPM	-0.128	-0.147	-0.138	-0.110
MS	0.187	0.161	-0.110	-0.071
RY	-0.525	-0.552	-0.203	-0.169
SAN	-0.241	-0.249	0.042	0.073
STAN	0.026	0	-0.121	-0.081
STT	-0.231	-0.225	0.123	0.127
TD	-0.392	-0.422	-0.177	-0.122
WBK	-0.493	-0.518	-0.188	-0.151
WFC	-0.161	-0.174	-0.089	-0.083
LYG	-0.240	-0.260	0.177	0.213
MUFG	-0.252	-0.290	-0.099	-0.046
AXA	-0.045	-0.045	-0.061	-0.054
$\lvert R_{t-1}\rvert$	0.161	0.164	-0.008	0
PTFSBD	0.066	0.061	0.005	0
PTFSFX	-0.022	0	-0.004	0
PTFSCOM	0.041	0.021	0.011	0
EMF	0.239	0	-0.005	0
ESF	0.100	0.040	-0.044	0
BD10RET	0.155	0.084	-0.046	0
BAAMTSY	-0.430	-0.332	0.062	0
MKT	-0.382	-0.130	0.023	0
SMB	-0.107	-0.085	0.041	0
HML	-0.055	-0.054	-0.011	0
MOM	-0.052	-0.044	-0.007	0

Table 7: Estimated regression parameters for the banks, obtained either from classical MLE or LASSO-type estimation procedures.

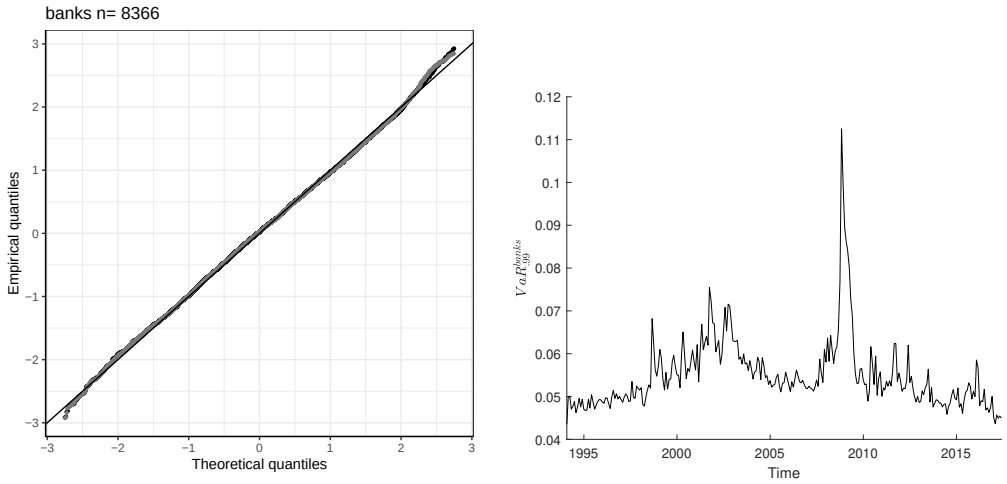

(a) (b)

Figure 4: (a) QQ-plot of the pseudo-residuals of the dynamic GP regression model for the banks' returns. Grey: residuals obtained from the classical MLE. Black: residuals obtained from the LASSO approach, followed by an additional MLE step with only the selected covariates. (b) Weighted VaR at level 99% (monthly average). The weights are the market value of the respective banks, expressed as a proportion of the total market value of our sample on a given day.

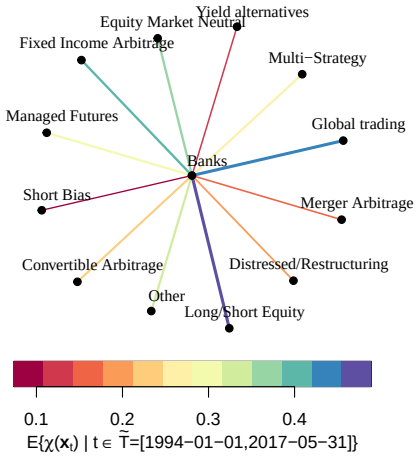

Figure 5: Unconditional estimate of the extremal connectedness between banks and the different investment styles.

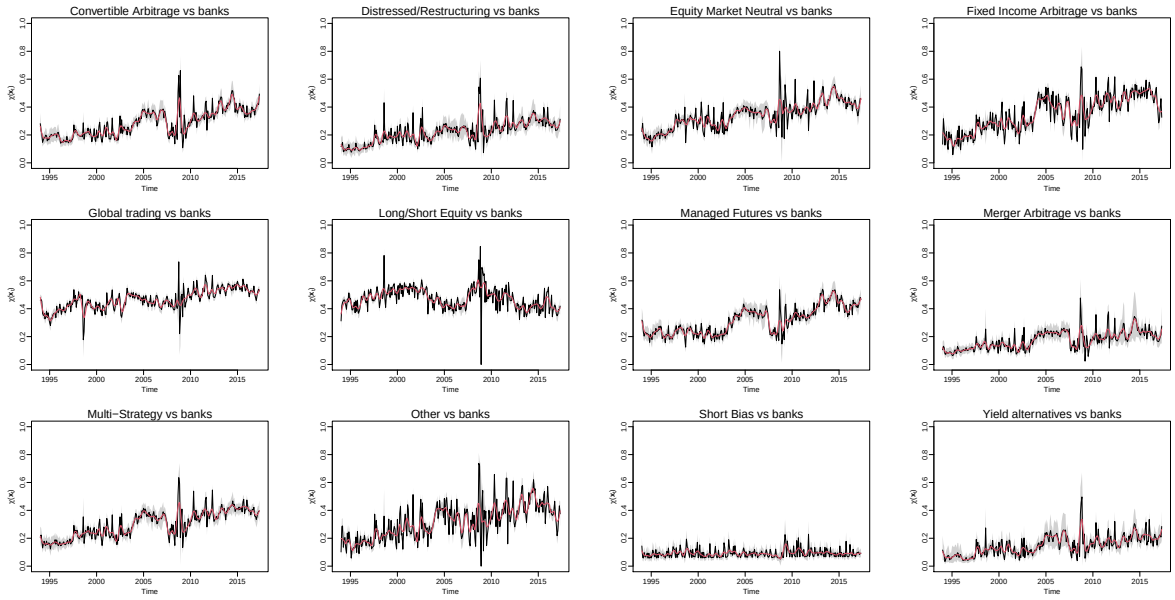

Figure 6: Estimates of the tail dependence over time between the banks and a given investment style. Asymptotic (pointwise) 95% confidence intervals are displayed in gray and a smoothed approximation using a lowpass moving average filter is represented in red.

first, we select financial institutions registered as "investment bankers/brokers and services stock trading". Then, we only keep the institutions listed on the NYSE, Euronext, the Tokyo Stock Exchange, and the SWX Swiss Exchange. Finally, we remove three institutions also listed as banks and that are used in our main analysis (Goldman Sachs, Morgan Stanley, and Credit Suisse). Our final sample consists of 21 institutions, listed in Table 8 (17 in the U.S., two in Europe, and two in Japan).

4.2 Marginal tail risk of brokers

In this section, we provide the estimated marginal tail risk regression parameters for our sample of 21 broker-dealers. As explanatory variables, we use brokers' fixed effects, the lagged absolute return $|R_{t-1}|$, the seven factors of Fung & Hsieh (2004) and the three factors of Carhart (1997)

Name	Ticker	Stock exchange
Ladenburg Thalmann Fin. Serv.	LTS	NYSE
Seaboard Corp.	SEB	NYSE
Cohen & Co.	COHN	NYSE
Waddell & Reed Financial	WDR	NYSE
Stifel Financial Corp.	SF	NYSE
Raymond James Financial	RJF	NYSE
Oppenheimer Holdings	OPY	NYSE
JMP group	JMP	NYSE
Intercontinental Exchange	ICE	NYSE
Greenhill & Co.	GHL	NYSE
GAMCO Investors	GBL	NYSE
GAIN Capital Holdings	GCAP	NYSE
Associated Capital Group	AC	NYSE
BlackRock	BLK	NYSE
Lazard	LAZ	NYSE
Charles Schwab Corp.	SCHW	NYSE
Jefferies Financial Group	JEF	NYSE
UBS	UBS	SWX
Natixis	KN	Euronext
Nomura	NOM	TSE
Daiwa Securities Group Inc.	DAW	TSE

Table 8: List of broker-dealers.

and Fama & French (1993) (size, value, and momentum). Classical MLE and LASSO-type estimators for the continuous covariates are reported in Table 9. Looking at the QQ-plot of the estimated model, the fit appears satisfactory, especially far in the tail (Figure 7, panel (a)). Similarly to what is done for the banks and hedge funds, we rely on our model to construct the weighted VaR at level $\alpha = 99\%$, over time and across all brokers, using the daily market values as weights. This quantity is displayed in Figure 7, panel (b), where we see an important peak during the financial crisis.

4.3 Connectedness with brokers

Using the estimated distribution, we transform the brokers' negative returns to the unit-Fréchet scale. For each month, the largest observations are matched with the largest monthly hedge funds' (rescaled) losses to form pairs of losses[3]. In Figure 8, we display the average connectedness between brokers and the various hedge funds' investment styles over the entire period of analysis, whereas in Figure 9, we display $\hat{\chi}_t^{brokers,l}$ over time. As for the banks, we find the investment styles *Global trading* and *Long short equity* to be strongly connected on average, whereas *Yield alternatives* and *Short bias* are weakly connected with brokers. Variations over time are limited. Overall, broker-specific connectedness is significant, indicating a sizeable likelihood of joint extreme losses between hedge funds and brokers. These results are in line with those obtained with the sample of large and systemically important banks. This is also consistent with the existence of broker-specific commonalities in hedge funds, as discussed in Chung & Kang (2016) and Kumar et al. (2020). In particular, under the contagion hypothesis discussed in Chung & Kang (2016) and which dominates in times of crisis, one would expect such a strong extremal connectedness.

Finally, we display several of the risk indicators proposed in the paper to measure the likelihood of spillovers between brokers and hedge funds: a broker-specific connectedness (the analogous of the bank-specific connectedness), as well as the $\Delta eCoVaR$ for four dates, with the same investment styles as references. These quantities are displayed in Figures 10 and 11. Regarding the total connectedness, we observe several phases: first, an increase from 1995 to (roughly) 2001, followed by a stable period. Contrary to the findings related to the bank connectedness, we do not witness an increase prior to the financial crisis. Connectedness remains stable until summer 2008, when it started increasing sharply up to February 2009, with the highest peak in October 2008. This is a result consistent with the contagion phenomenon discussed by Chung & Kang (2016), where brokers act as propagators of liquidity shocks to their clients. After a fall in March 2009, connectedness progressively increases up to 2013, reaching a value around .4 at

[3]This matching approach implies that the extremal connectedness is assumed constant within a given month

Factor	$\hat{\boldsymbol{\beta}}_0^{\sigma}$ (MLE)	$\hat{\boldsymbol{\beta}}_0^{\sigma}$ (LASSO)	$\hat{\boldsymbol{\beta}}_0^{\xi}$ (MLE)	$\hat{\boldsymbol{\beta}}_0^{\xi}$ (LASSO)
KN	-3.989	-3.978	0.143	0.154
DAIWA	-0.172	-0.164	0.005	-0.004
JEF	-0.368	-0.344	0.093	0.065
LAZ	-0.151	-0.164	-0.155	-0.172
NOMU	-0.095	-0.090	-0.044	-0.041
SCHW	-0.138	-0.123	-0.025	-0.037
UBS	-0.041	0.004	-0.074	-0.116
BLK	-0.218	-0.214	-0.084	-0.080
AC	-0.399	-0.665	-0.323	-0.285
GCAP	0.319	0.108	0.145	0.178
GBL	-0.046	-0.064	0.022	0.058
GHL	-0.157	-0.168	-0.073	-0.100
ICE	-0.027	-0.125	-0.027	0.033
JMP	0.049	-0.124	-0.261	-0.215
OPY	0.051	0.049	-0.091	-0.089
RJF	-0.038	0	-0.146	-0.173
SF	-0.059	-0.070	-0.134	-0.141
WDR	-0.006	0	-0.213	-0.217
COHN	0.272	0.077	0.142	0.189
SEB	0.074	0.040	-0.075	-0.055
LTS	0.449	0.424	0.016	-0.005
$\lvert R_{t-1}\rvert$	0.158	0.119	-0.020	0
PTFSBD	0.015	0	0.036	0.025
PTFSFX	0.022	0	-0.047	0
PTFSCOM	0.017	0	0.062	0.038
EMF	-0.121	-0.036	0.030	0
ESF	0.091	0	-0.025	0
BD10RET	0.152	0	-0.048	0
BAAMTSY	-0.343	-0.223	0.054	0
SMB	-0.082	0	0.015	0
HML	-0.055	0	0.022	0
MOM	-0.045	0	0.003	0

Table 9: Estimated regression parameters for the broker-dealers, obtained either from classical ML estimation or LASSO-type estimation procedures.

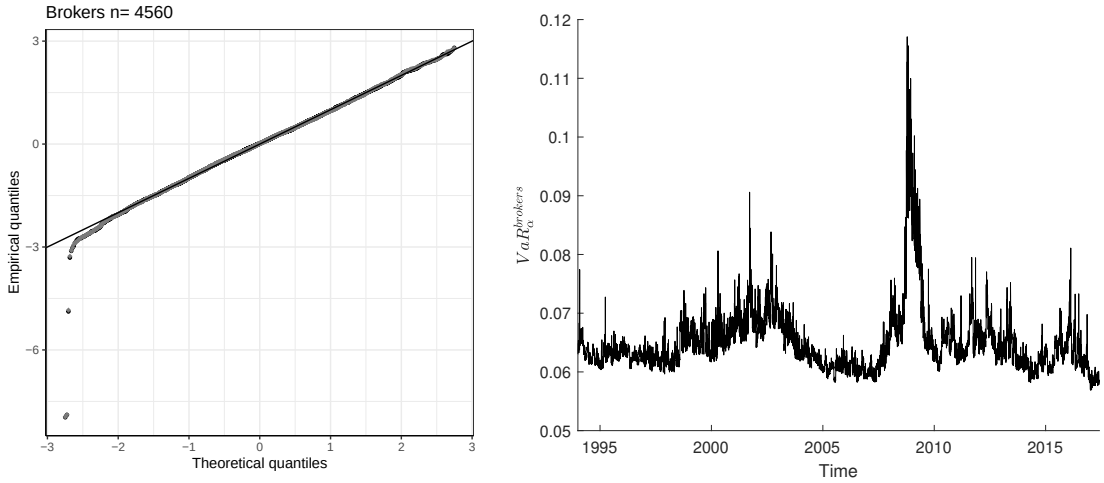

(a) (b)

Figure 7: (a) QQ-plot of the pseudo-residuals of the dynamic GP regression model for the brokers' returns. Grey: residuals obtained from the classical MLE. Black: residuals obtained from the LASSO approach, followed by an additional MLE step with only the selected covariates. (b) Weighted (total) VaR at level 99% for the sample of brokers. The weights are the market value of the respective brokers, expressed as a proportion of the total market value of our sample on a given day.

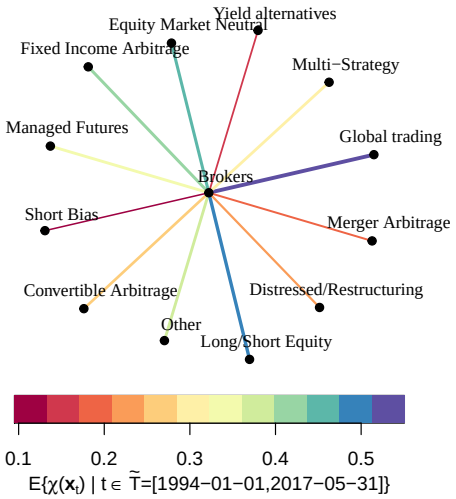

Figure 8: Unconditional estimate of the extremal connectedness between brokers and the different investment styles.

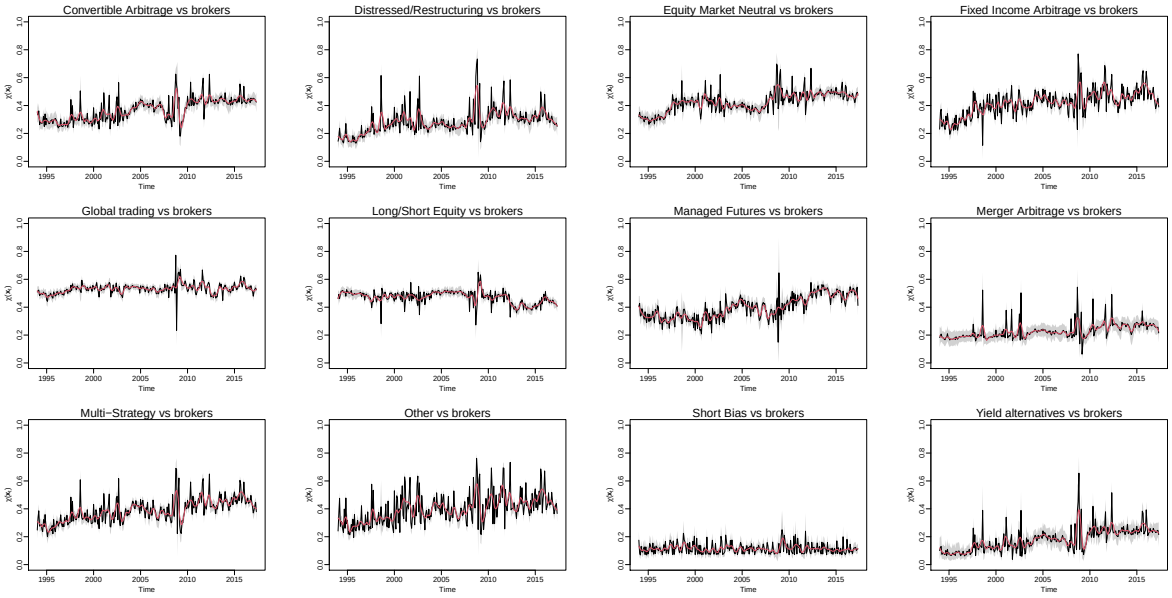

Figure 9: Estimates of the tail dependence over time between the brokers and a given investment style. Asymptotic (pointwise) 95% confidence intervals are displayed in gray and a smoothed approximation using a lowpass moving average filter is represented in red.

the end of our sample. Finally, regarding $\Delta eCoVaR$, we observe relatively few discrepancies in normal times (i.e., July 2007) between the reference styles displaying the smallest and highest average connectedness (namely *Short bias* and *Global trading*). However, during the crisis, the risk contribution of *Global trading* is significantly larger than the one of *Short bias* (15% against 20% in October 2008), a result that can be connected with both the information connection hypothesis of Kumar et al. (2020) and the contagion hypothesis of Chung & Kang (2016), suggesting both that equity funds (in particular those invested in emerging markets) share a special connection with their brokers.

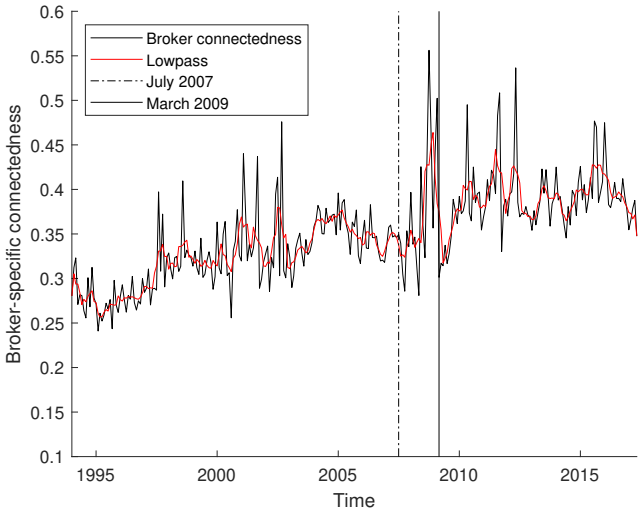

Figure 10: Broker-specific connectedness $\tilde{\chi}_t^{brokers}$ (black). Smoothed approximation using a lowpass moving average filter is represented in red.

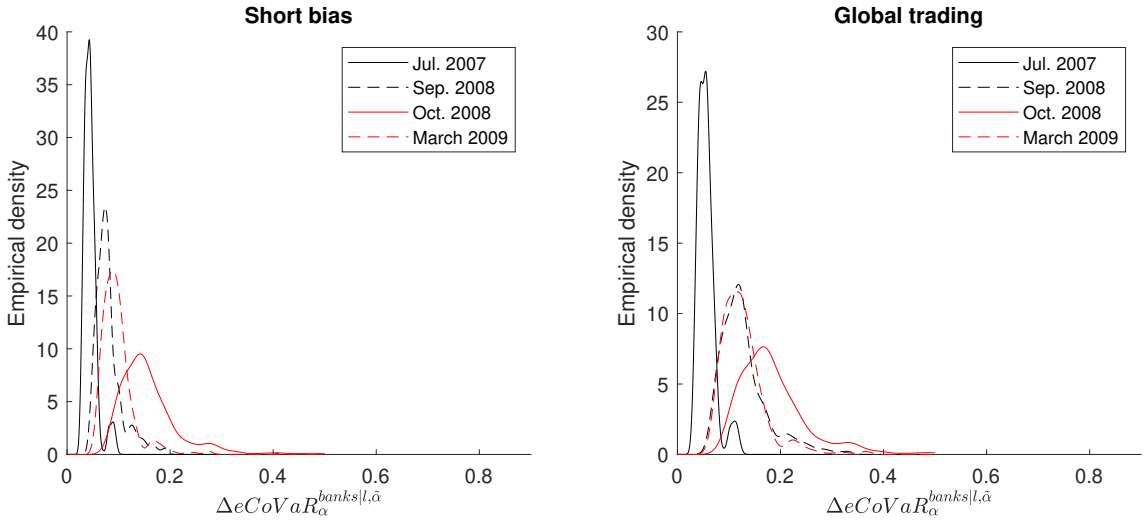

Figure 11: Empirical density of the brokers' RC for *Short bias* and *Global trading* at four different dates: July 2007, September 2008, October 2008, and March 2009. We fix $\alpha = \tilde{\alpha} = 0.975$.

5 Simulation study

5.1 Capturing heteroscedasticity at the fund's level

In this section, we report the results of a simulation study emphasizing the suitability of our approach to deal with heteroscedasticity at the fund level. A legitimate question regarding our

marginal modeling relates to the impact of fund-level heteroscedasticity on the estimation. To control for this effect when estimating the marginal tail risk, we include the absolute lagged returns of the funds in the set of predictors, in line with the findings of Trapin (2017), Bee et al. (2018), and Bee & Trapin (2018). This solution was found preferable to the use of a fund-level volatility proxy. To emphasize the suitability of this approach to deal well with a GARCH-type structure of the volatility without including fund-level volatility estimates, we conduct several simulation scenarios where the tail distribution is estimated through a dynamic GPD with non-stationary scale parameter and constant shape (a set-up in line with our findings where our LASSO approach retains almost no covariate in the shape parameter, and with Mikosch & Starica (2000) who show that the tail index associated with a GARCH(p, q) process is constant). The considered simulations schemes are the following:

1. We simulate a single time series of length $T = 10,000$ from a classical GARCH(1,1) model, then select the 5% smallest observations, and apply the dynamic EV regression approach to estimate the tail distribution. Beforehand, we multiply every return by -1 to work with losses. As explanatory variables, we use for each extreme observation the absolute return from the previous period.

2. We simulate (independently) 1000 time series of length $T = 100$ following two different GARCH structures (500 series each). Then, we select the 5% smallest observations of the complete panel. Similarly to the first simulation, we estimate the dynamic EV regression model with the lagged Realized Measure of Volatility (RMV), in each time series, as explanatory variable.

3. We repeat the simulation set-up (2) but instead of using a global threshold, we estimate a time-varying threshold via quantile regression, using a polynomial function of time.

4. Finally, we repeat again the set-up (2), and use the theoretical quantile of each observation as a threshold: if a return is smaller than the 5% quantile of its conditional distribution, it is retained as an exceedance.

In Table 10, we detail the parameters of the GARCH models and the distributional assumptions made for the different data generating processes (DGP). To assess the goodness-of-fit of the dynamic EV regression models, we look at the QQ-plots of the Gaussian pseudo-residuals obtained via probability integral transform. We repeat the simulation 200 times, and compute the residuals' quantiles, for probabilities ranging between .001 and .999. In Figure 12, we display the median estimates, as well as the Monte Carlo percentile confidence intervals at level 5%, i.e., the quantiles at level .025 and .975 across simulations. We see that we fit well the distribution of the observations far in the tail in all setups.

For setup (4) where the effect of threshold selection has been neutralized by the use of the true quantile, we also compute 99% quantile estimates of the loss distribution for each observation at each point in time, using the dynamic EV approach. We obtain perfect quantile coverage probabilities with our approach. Finally, we compute the mean squared forecast error for the predicted quantile at level 99%. We compare our results with those obtained using as explanatory variables either the true lagged standard deviation, the true contemporaneous standard deviation or their estimated counterparts. Estimates are obtained by fitting GARCH(1,1) models to the time series of returns. In Figure 13, we display the boxplots of the sum of squared errors (SSE) for the various specifications. We see that using the true values of the volatility process, we obtain the smallest SSE among all specifications. However, the model based on the RMV largely outperforms the one based on estimated volatility.

Thus, aside from the theoretical arguments raised by Bee et al. (2019) for non-stationary volatility processes (a likely feature of the data due to the dynamic investment strategy pursued by hedge funds), it appears also that the use of lagged absolute returns as a predictor in our dynamic EV regression model offers the best compromise between goodness-of-fit of the tail distribution, correct empirical coverage and overall quantile estimation.

Simulation set-up	ω	α	β	Distribution
DGP 1	.0001	.93	.05	Student, $\nu = 5$
DGP 2 (a)	.0001	.9	.05	Student, $\nu = 5$
DGP 2 (b)	.0001	.8	.1	-
DGP 3 (a)	.0001	.85	.08	Student, $\nu = 5$
DGP 3 (b)	.0001	.92	.05	- -
DGP 4 (a)	.0001	.9	.05	Student, $\nu = 5$
DGP 4 (b)	.0001	.8	.1	-

Table 10: Parameters used in the different simulation setups. The quantities ω, α, and β denote the constant, auto-regressive, and moving-average parameters, respectively, of the GARCH process. For DGP 2 to 4, we combine two different processes. All innovations are simulated from a standardized Student distribution with five degrees of freedom.

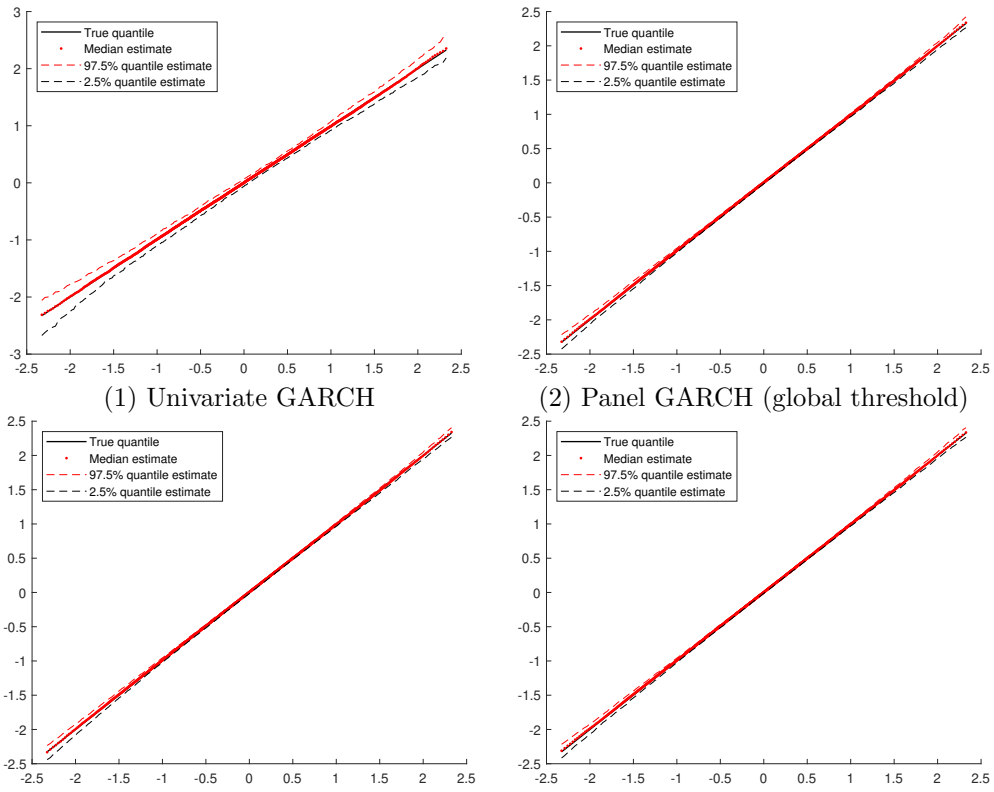

(1) Univariate GARCH (2) Panel GARCH (global threshold)

(3) Panel GARCH (quant. reg. threshold) (4) Panel GARCH (theo. quantile)

Figure 12: QQ-plots of the pseudo residuals obtained with the dynamic EV regression approach.

5.2 Modeling tail dependence in a two-step approach

Here, we illustrate the adequate performances of our two-step approach in estimating the strength of the tail dependence under a dynamic setting.

We simulate from the t-copula model that exhibits tail dependence (as opposed to the Gaussian copula) with covariate-dependent margins. Then, we apply our two-stage procedure with the semi-parametric marginal transformation described by equation (15) in a first step, and the estimation of the tail dependence performed in a second step. The tail dependence modeling consists in fitting the Hüsler–Reiss angular density to the pseudo-angular observations (of the first step) with a radial component exceeding a high threshold, set here at the 95% quantile of the radial variable; see Section 2.2 for details.

To assess the propagation of the impact of misspecification and parameter uncertainty of the

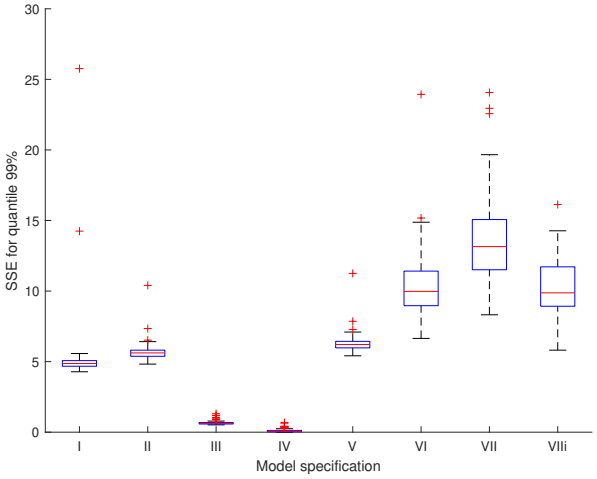

Figure 13: Boxplots of the sum of squared errors (SSE) for the quantile 99%, obtained with various specifications. I and II: RMV_{t-1} and $\log(RMV_{t-1})$. III and IV: $\log(\sigma_{t-1})$ and $\log(\sigma_t)$. V: uninformative process x_{t-1} following an independent GARCH process. VI, VII and VIII: $\log(\hat{\sigma}_{t-1})$, $\log(\hat{\sigma}_t)$ and $(\mathrm{RMV}_{t-1}, \log(\hat{\sigma}_{t-1}))$.

margins in the dependence modeling, we compare the estimated coefficient of tail dependence χ resulting from the estimation of the t-copula based on the pseudo-uniform observations, i.e., the semi-parametrically transformed marginal observations, with the true value of χ under the t-copula model, i.e.,

$$\chi = 2t_{\nu+1}(-\sqrt{\nu+1}\sqrt{1-\rho}/\sqrt{1+\rho}),$$

where ν and ρ represent the degree of freedom and the correlation parameter associated with the t-copula, respectively. Additionally, we compare these two quantities to the estimated coefficient of tail dependence obtained by assuming a Hüsler–Reiss copula for the tail dependence. Such comparison allows quantifying the effect of the double misspecification of the model (the margins are captured semi-parametrically and the dependence is modeled using an extreme value copula in the tails).

We simulate 2000 observations from this model, with a degree of freedom $\nu = 4$ and different strengths of dependence, captured by the correlation parameter ρ. Regarding the margins, we consider the following two settings:

- The margins are Student's t distributed with a degree of freedom

  $$\nu(x) = 4 + \log(1 + x)$$

  depending on a deterministic covariate x, different for each margin. Here, the marginal distribution is in the maximum domain of attraction of a GEV and the use of the GP distribution (in the first step) holds only approximately for any high finite threshold.

- The margins are GEV distributed with location and shape equal to one and a scale parameter

  $$\sigma(x) = \log(1/2 + x)$$

  depending on a deterministic covariate x, different for each margin. Here, the use of the GP distribution holds exactly for any finite threshold.

Figure 14 displays the estimated tail dependence coefficient for both settings, different correlations, and 300 replicates.

Comparing the estimated tail dependence coefficient resulting from fitting the correctly specified t-copula, we notice that the semi-parametric marginal transformation seems to have little to no impact on the estimation of the strength of tail dependence. This is valid for both covariate-dependent marginal settings where the true underlying marginal distribution is either in the maximum domain of attraction of an extreme value distribution, i.e., the marginal $t-$distribution, or is an extreme value distribution itself, i.e., the marginal GEV distribution. Note however that

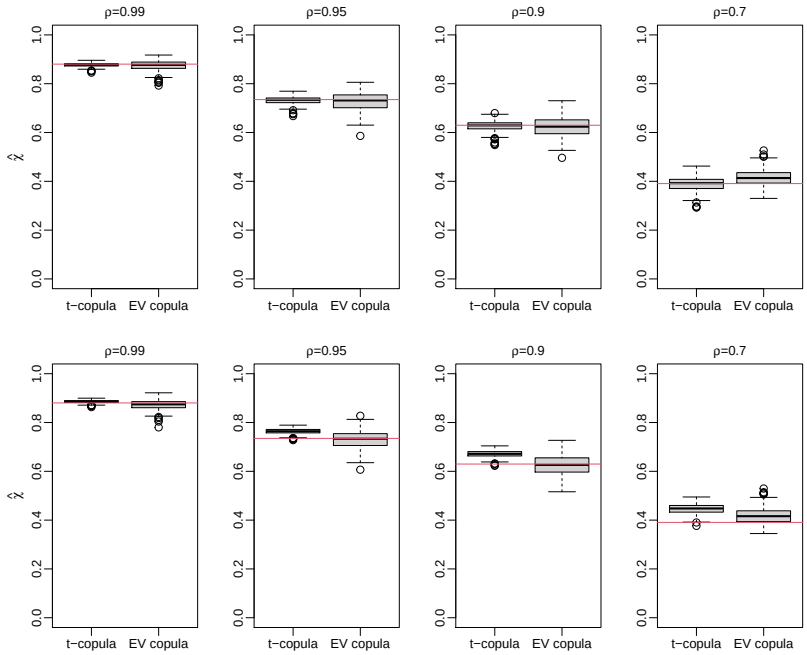

Figure 14: Boxplots of the estimated coefficient of tail dependence under different dependence strengths dictated by the correlation coefficient ρ of the t-copula. Top panels display the results for the Student's t-margins and bottom panels for the GEV margins.

we observe a slight bias when dependence is rather weak. This is due to the fact that under such setting, inference about tail dependence involves more observations that are extreme only in one margin and are thus rank-transformed.
Comparing the estimated tail dependence coefficient resulting from fitting the Hüsler–Reiss angular density to the semi-parametrically transformed observations (to unit-Fréchet scale) with a radial component exceeding a high threshold, we notice a slight upward bias when tail dependence is rather weak. This bias is addressed in Mhalla et al. (2019) and is expected as the angular density is valid only asymptotically and a finite radial threshold is needed in practice.

References

Agarwal, V., Ruenzi, S. & Weigert, F. (2017), 'Tail risk in hedge funds: A unique view from portfolio holdings', *Journal of Financial Economics* **125**(3), 610–636.

Bee, M., Dupuis, D. J. & Trapin, L. (2018), 'Realized extreme quantile: A joint model for conditional quantiles and measures of volatility with evt refinements', *Journal of Applied Econometrics* **33**(3), 398–415.

Bee, M., Dupuis, D. J. & Trapin, L. (2019), 'Realized Peaks over Threshold: A Time-Varying Extreme Value Approach with High-Frequency-Based Measures', *Journal of Financial Econometrics* **17**(2), 254–283.

Bee, M. & Trapin, L. (2018), 'Estimating and forecasting conditional risk measures with extreme value theory: A review', *Risks* **6**(2).

Carhart, M. M. (1997), 'On persistence in mutual fund performance', *The Journal of Finance* **52**(1), 57–82.

Chung, J.-W. & Kang, B. U. (2016), 'Prime Broker-Level Comovement in Hedge Fund Returns: Information or Contagion?', *The Review of Financial Studies* **29**(12), 3321–3353.

Fama, E. & French, K. (1993), 'Common risk factors in the returns on stocks and bonds', *Journal of Financial Economics* **33**(1), 3–56.

Fung, W. & Hsieh, D. (2004), 'Hedge fund benchmarks: A risk-based approach', *Financial Analysts Journal* **60**(5), 65–80.

Hale, G. & Lopez, J. A. (2019), 'Monitoring banking system connectedness with big data', *Journal of Econometrics* **212**(1), 203–220.

Hambuckers, J., Groll, A. & Kneib, T. (2018), 'Understanding the economic determinants of the severity of operational losses: A regularized generalized Pareto regression approach', *Journal of Applied Econometrics* **33**(6), 898–935.

Hüsler, J. & Reiss, R.-D. (1989), 'Maxima of normal random vectors: Between independence and complete dependence', *Statistics & Probability Letters* **7**(4), 283–286.

Kumar, N., Mullally, K., Ray, S. & Tang, Y. (2020), 'Prime (information) brokerage', *Journal of Financial Economics* **137**(2), 371–391.

Mhalla, L., de Carvalho, M. & Chavez-Demoulin, V. (2019), 'Regression-type models for extremal dependence', *Scandinavian Journal of Statistics* **46**, 1141–1167.

Mikosch, T. & Starica, C. (2000), 'Limit theory for the sample autocorrelations and extremes of a garch (1, 1) process', *The Annals of Statistics* **28**(5), 1427–1451.

Trapin, L. (2017), 'Can Volatility Models Explain Extreme Events?', *Journal of Financial Econometrics* **16**(2), 297–315.